Metals Materials And Processes, 2000, Vol. 12, No. 2 & 3, pp. 143 - 160.

KINETICS OF SOME DISPLACIVE SOLID → SOLID PHASE TRANSFORMATIONS UNDER ISOBARIC-ISOTHERMAL CONDITIONS

Murali Mohan
Materials Science Division, National Aerospace Laboratories, Bangalore 560 017

(Received 10 January 2000)

Abstract : The research activities in the area of the kinetics of pressure induced solid → solid phase transformations are discussed in this paper. The experimental techniques for obtaining the kinetics data under isobaric-isothermal conditions using the resistometric method are described. The transformations investigated are the $\alpha \rightarrow \omega$ in Ti, fcc → bcc in Yb and hcp → fcc in TI. These transformations exhibit features characteristic of a thermally activated nucleation and growth behaviour. The activation volume, the activation entropy and the activation enthalpy obtained from the analysis of the kinetics data are compared. The implications of the kinetics data on the transformation start pressure and the thermodynamic equilibrium pressure are discussed.

Keywords: phase transformations, kinetics, thermodynamics

1. INTRODUCTION

Most changes under pressure in the physical properties of solids are brought about by the fact that atoms in solids come closer under pressure. The crystal structure stable under normal conditions of temperature (T) and pressure (p) may develop instability due to the fact that under pressure some other atomic arrangement has a lower free energy. A continuously increasing pressure will take such a solid to a pressure at which the free energies of the low and the high pressure phases (respectively denoted as phase A and phase B) are equal. This pressure is termed the thermodynamic equilibrium press p_o. A pressure induced phase transformation from A → B becomes observable at any applied pressure $p_f > p_o$, where p_f is the start pressure of the forward transformation A → B, and lies in the stability region of B: $(p_f - p_o)$ is termed the over-pressure. Similarly, when the pressure is reduced from a value where only B is present A does not reappear until a pressure $p_r < p_o$ is reached. p_r is termed the start pressure of the reverse transformation B → A and $(p_r - p_o)$ is the under-pressure. The requirement of an over-pressure (under-pressure) to drive the transformation A → B (B → A) implies that the phase transformation A ↔ B exhibits a hysteresis. The hysteresis is a consequence of the fact that the transformation faces an activation energy barrier ΔG^*. The thermodynamic driving force for the transformation A → B is $(p_f - p_o)\ \Delta V_f$ where ΔV_f is the fractional volume change associated with the transformation. The new phase B develops at a finite rate only under non equilibrium conditions i.e., $p_f > p_o$ because at p_o the thermodynamic driving force for the transformation is zero. Since both the activation energy barrier and the thermodynamic driving force are pressure dependent the kinetics of the A → B phase transformation depends largely on the over-pressure, and likewise the kinetics of the B → A transformation depends on the under-pressure.

A pressure induced structural transformation is always accompanied by an increase in density (negative ΔV_f) and is essentially first order, and governed by the Clausius - Clapeyron equation. Further, pressure-induced structural transformations occurring at room temperature (low k_BT) are usually of the displacive type and the structural changes involve only small atomic displacements. The transformations are relatively rapid and are

generally reversible. On the other hand, pressure-induced structural phase transformations can also be of the reconstructive type which usually occur at high temperature and the structural changes are brought about by the breaking and reforming of the bonds. The reconstructive type transformations are generally irreversible. The displacive type phase transformations are interface controlled and the reconstructive types are diffusion controlled. This paper deals with the pressure and temperature dependence of the kinetics of a few displacive type of phase transformations.

1.1 Background information

Ideally, a microscopic observation of the transforming specimen will lead to a clear understanding of the processes underlying the transformation. There are experimental difficulties in making such a direct observation of the transforming specimen under pressure. However, microscopic observations are possible on the pressure quenched specimens transformed to different extents, if the high pressure phase can be retained metastably at atmospheric pressure. In view of these difficulties, the progress of a pressure induced solid-solid phase transformation is followed by indirect methods. These involve, the recording with time of the changes in electrical resistivity, volume, capacitance, optical absorption, x-ray scattering, Raman scattering associated with the transformation and from these the kinetics data, i.e., fraction transformed as a function of time, are obtained at different over-pressures. For an unambiguous interpretation of these data it is desirable that the data are obtained under isobaric-isothermal conditions.

A detailed review of the earlier studies on the kinetics of pressure induced phase transformations in solids will not be attempted here as several review papers[1-5] already exist in literature. However, the following limitations of the earlier studies are pointed out. The emphasis in the earlier studies has been mainly on the increase in the rate of transformation with increase in pressure. In most of these studies, quantitative kinetics data have not been obtained systematically as a function of increasing over-pressure. Even when such data have been obtained, the range of over-pressures is limited and truly isobaric conditions have not been maintained while monitoring the progress of the transformation. The following considerations bring out the importance of employing higher pressurization rates in obtaining the kinetics data under isobaric conditions. In principle, a pressure induced phase transformation can occur at any pressure p higher than p_o. The start pressure of the transformation is determined by the rate of pressurization and the rate of transformation at that pressure. If the rate of pressurization is higher than the rate of transformation then values of p far removed from p_o can be reached before the onset of transformation can be detected. This is the first step in achieving isobaric conditions and the next is to maintain the pressure constant at the desired value during the progress of the transformation. Further, higher pressurization rates extend the range of over-pressures over which the kinetics data can be obtained.

A comparison of some of the methods that have been employed in the earlier studies to obtain the kinetics data of pressure induced phase transformations with a view to pointing out their merits and drawbacks will be in order at this stage. The transformations resulting in quenchable phases can be monitored by x-ray diffraction technique. This involves holding the sample at a given T and p for different t and quenching it to room temperature and one atmosphere. The fraction of the retained high pressure phase is determined at one atmosphere by x-ray diffraction technique. This method has the disadvantages in that it is cumbersome and further that the exposure time is large. The high intensity x-ray sources such as synchrotron radiation source enables to record diffraction patterns from samples under pressure in a few minutes. Thus, it is possible to determine the fraction

transformed as a function of time by first pressurizing the sample, and later carrying out *in situ* x-ray diffraction analysis. However, the x-ray methods of obtaining the kinetics data are less precise. The methods based on the measurement of volume and resistance change associated with the transformation, can detect transformed fraction down to half per cent. In these methods, the measurements can be carried out continuously, and hence these are suitable for studying faster kinetics. A piston-cylinder high pressure setup is ideally suited for the measurement of volume change as a function of time during the progress of the transformation and the kinetics data can be directly obtained from the time dependence of the volume change. A large volume of the specimen, typically $1cm^3$, will lead to an increased sensitivity in the measurement of the volume change. But, as the transformation proceeds, the large size of the specimen also leads to a large drop in pressure. Unless the pressure is maintained constant, the kinetics data cannot be obtained under isobaric conditions. Further, the highest pressure in a piston-cylinder apparatus is limited to 5 GPa. The resistometric methods are the most convenient for obtaining the transformed fraction in conducting samples. These methods require small samples (typically $5x0.5x0.05\ mm^3$) and therefore opposed anvil devices can be used to pressurise the specimen easily up to 15 GPa; small sample volume will lead to small pressure drop from the set value during the progress of the transformation and hence isobaric conditions are maintained. We have deviced an experimental setup[6] to step-load the opposed anvil system so that the desired values of specimen pressure can be reached before the onset of transformation can be detected and the progress of the transformation can be monitored under truly isobaric-isothermal conditions. All the earlier studies employing the resistometric method assume that the transformed fraction at any instant, t, is directly proportional to the resistance change at t. This is true only if the electrical resistance of the phases involved in the transformation lie in a series arrangement. This approximation is not generally valid. Clearly, the transforming specimen is an intimate random mixture of both the phases. So an appropriate model for the effective electrical conductivity of the mixture of two phases should be used to obtain the transformed fraction-time data from the resistance-time data. We have examined[7] the variations in the values of the transformed fraction resulting from using different models of effective electrical conductivity of a two-phase mixture and find that these values differ appreciably when the magnitude of the resistance change at the transformation is larger. Further, we find that the Landauer model[8], which assumes a homogeneous random mixture of the constituent phases in obtaining the electrical conductivity of a two-phase mixture is best suited for obtaining the kinetics data from the resistometric data.

We have systematically investigated the pressure and temperature dependence of the kinetics of hcp(α) → hexagonal (ω) transformation in Ti, fcc ↔ bcc transformation in Yb and the hcp → fcc transformation in Tl under truly isobaric-isothermal conditions. The experimental techniques, the methods of data recording and processing and detailed analysis of the kinetics data have been described in earlier publications [9-17]. The salient features of these investigations are briefly summarised in this paper.

2. EXPERIMENTAL DETAIL

2.1 Specimens for kinetics studies

The starting materials for the resistance measurements are Marz grade Ti wire, 0.125 cm in diameter (Materials Research Corporation USA), Yb lumps, 99.9% pure (Rare Earth Products Ltd USA) and Tl shots, 99.999% pure (Atomergic Chemetals Corporation USA).

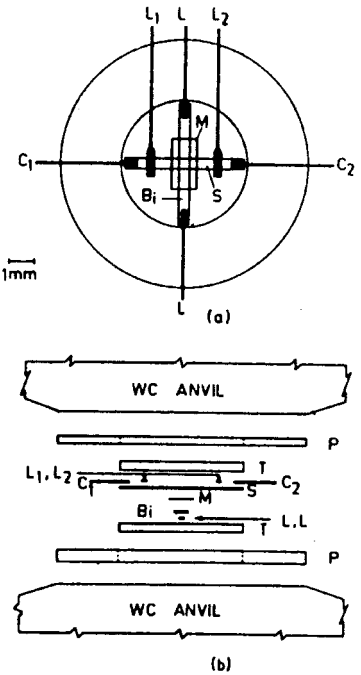

Fig. 1.(a)High pressure resistivity cell with the specimen in a four lead configuration (b) Stacking sequence of the various components of the cell p,p-pyrophyllite gasket, T,T-talc pressure transmitters, S-specimen, C_1, C_2 current leads, L_1, L_2 voltage leads.

These are flattened by pressing them between hardened and ground steel plates and from these specimens measuring 5x0.5x0.05 mm^3 are cut, and thoroughly cleaned.

2.2 High pressure set up and the resistivity cell

A tungsten carbide opposed anvil setup (12.7 mm anvil face) powered by a 100 ton hydraulic ram with pyrophyllite gasket (a stack of 2 gaskets each measuring 12.5 mm od, 5 mm id and 0.4 mm thickness) and talc (2 discs each measuring 5 mm diameter and 0.36 mm thickness) as a pressure transmitter is used to pressurize the specimen. The resistance of the specimen is measured using a four-lead arrangement (Fig.1). For this, a constant d.c current (up to 100 mA) is maintained through the specimen, and the output across the voltage leads is recorded with a strip chart recorder (Rikadenki R-50 series, sensitivity 1 mV full scale).

The relation between the applied load L and the specimen pressure, p, is very nearly linear[5] with a pressure amplification factor of 2.4. For a given pair of anvils, the L-p relation mainly depends on the gasket thickness. A careful control over the dimensions of the gasket and the pressure transmitting discs in each run gave a highly reproducible (within 5%) L-p relation. The uncertainty in the specimen pressure is further reduced (~1%) by determining the L-p relation independetly in each run. For this, a Bi specimen (3x0.5x0.05 mm^3) is placed perpendicular to the specimen under study and the **I** $\rightarrow$ **II** (2.55 GPa) and **III** $\rightarrow$ **V** (7.7 GPa) transformations in Bi are detected using a two lead arrangement. The details of the high pressure resistivity cell and the lead arrangements have been described elsewhere[4,5,11].

Radial pressure gradients are invariably present in the resisitivity cell because a solid is used as a pressure transmitter. A theoretical analysis of the pressure distribution in a compressible gasket placed between the opposed anvils is quite complicated. We have determined the radial pressure distribution experimentally[16]. It is found from these studies that (1) the radial pressure distribution is symmetric about the centre (b) the pressure is maximum at the centre of the cell and decreases radially along the length of the specimen (c) for a given gasket thickness, the pressure gradient increases with radial distance and the radial pressure differences at a given location increase with p (d) the radial pressure differences increase with increasing gasket thickness and so also is the pressure amplification factor (e) L-p relation becomes progressively non-linear with increasing gasket thickness. These results suggest that the thickness of the gasket has to be optimised compromising between the radial pressure differences on one hand and the pressure amplification factor on the other. In our experiments, the gasket thickness is 0.8 mm and the distance between the voltage leads (transformation region of interest) never

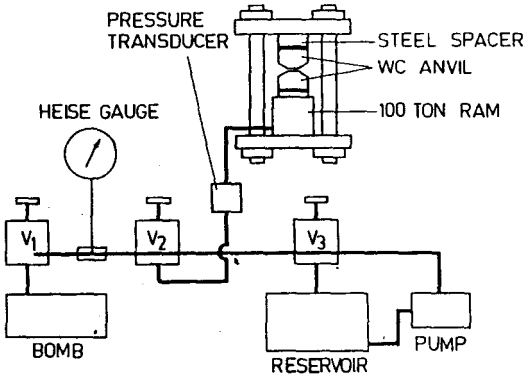

Fig. 2. Schematic diagram of the step-loading arrangement

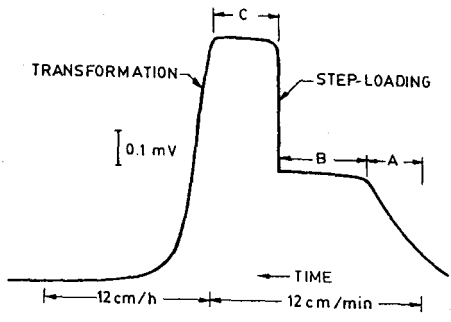

Fig. 3. Typical variation of the voltage across the Yb-specimen during pressurization

exceeded 1.0 mm. The estimated radial pressure differences over this length are 0.015 GPa at 2.55 GPa and 0.05 GPa at 7.7 GPa.

2.3 Step-loading arrangement

The step loading of the opposed anvil system is achieved using an arrangement shown schematically in Fig.2 [6]. The high pressure bomb (70 MPa), the hydraulic ram and the reservoir can be isolated by closing the valves $\mathbf{V}_1$, $\mathbf{V}_2$, and $\mathbf{V}_3$ respectively. The hydraulic ram is first pressurized to p_i by closing valve $\mathbf{V}_3$ and opening $\mathbf{V}_1$ and $\mathbf{V}_2$; the bomb also gets pressurized to p_i simultaneously. The ram is isolated by closing $\mathbf{V}_2$ and the bomb is pressurized to p_b ($p_b > p_i$). When $\mathbf{V}_2$ is suddenly opened, the ram pressure experiences a jump and finally reaches p_f such that $p_i < p_f < p_b$. The rapid pressurization leads to a specimen pressurization at a rate 10 GPa s^{-1} as against a pressurization rate of 0.1 GPa min^{-1} normally employed in the continuous monitoring of the resistance-pressure data. It is important to note that the opposed anvil device can be operated in the normal manner by closing $\mathbf{V}_1$ (which isolates the bomb). The normal and rapid rates of pressurization of the specimen can be empoyed at any stage during a kinetics experiment. That the L-p relation obtained under continuous loading remains valid even under an intermediate step loading has been examined[6] extensively. The specimen temperature is estimated to increase at a rate1.45 K/GPa during step loading and decreases to room temperature within 1 second.

2.4 Sequence of steps in a kinetics experiment

A typical record of the variation with time of the voltage across the Yb specimen during an actual experiment is shown in Fig.3. The specimen is pressurized at a rate 0.1 GPa min^{-1} up to 2.55 GPa as indicated by the Bi **I** → **II** transformation. Region A corresponds to the increase of resistance of the fcc phase during the continuous pressurization. The end of region A marks the point where it is planned to step-load the opposed anvil setup. The region B indicates the pause during the pressurization of the bomb; the constancy of the voltage across the specimen denotes that the specimen pressure is held constant at 2.55 GPa. The specimen is now pressurized at a rate 10 GPa s^{-1} to desired pressures in the range 3.3 to 4.6 GPa and held constant. The sudden increase in the voltage across the specimen is the normal increase in the resistance of the fcc phase arising from the pressure step. The region C marks the period over which the specimen voltage remains constant even after the desired pressure is reached. Beyond C, the progress of the fcc →

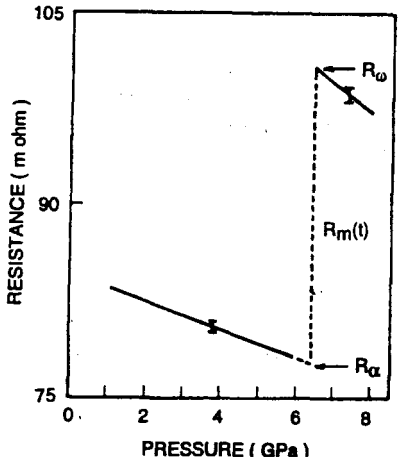

Fig. 4(a) Resistance of the Ti-specimen as a function of pressure; the discontinuous increase indicates $\alpha \rightarrow \omega$ the transformation.

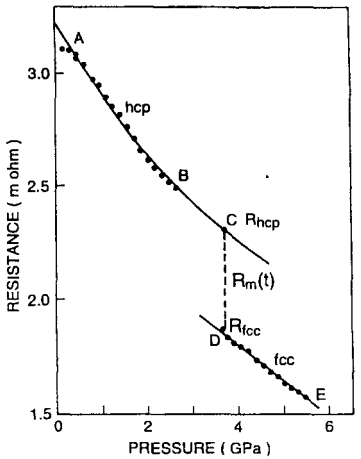

Fig. 4(b). Resistance of the Tl-specimen as a function of pressure, the drop indicates the hcp $\rightarrow$ fcc transformation.

bcc transformation, marked by a large decrease in voltage, at a constant pressure is seen. The time dependence of the transformation is recorded until it ran to completion. The transformation is considered complete when no further decrease in the specimen voltage is observed. That the fcc $\rightarrow$ bcc transformation is complete at this stage is further confirmed by increasing the specimen pressure at a rate 0.1 GPa min^{-1} and continuously monitoring the changes in the specimen voltage. The voltage across the specimen marginally decreased with increase in pressure; the pressure coefficient of resistance was characteristic of the bcc phase. Similar records of the resistance-time data associated with the $\alpha \rightarrow \omega$ transformation in Ti and the hcp $\rightarrow$ fcc transformation in Tl at a desired value of specimen pressure are obtained.

In all the experiments, the rapid pressurization of the specimen ensured that the desired pressures are reached before the onset of transformation can be detected. Further, the hydraulic pressure corresponding to desired values of specimen pressure is held constant (one part in 200) over the entire duration of the transformation. The changes in the specimen pressure, if any, arising from the gasket relaxation under a constant applied load during a waiting period of over 2 days are estimated in separate experiments with the manganin specimen[16] and it is found that the pressure increase, if any, is 0.03 GPa.

2.5 Salient features of the present method

The following points about the experimental procedure discussed so far are noteworthy: (1) isobaric conditions are established before the onset of the transformation (2) the desired pressure is held constant (applied load: 1 part in 200) during the transformation (3) radial pressure differences over the region of interest are ~0.05 GPa (4) the uncertainty in the specimen pressure is ±0.05 GPa at 5 GPa and ±0.1 GPa at 10 GPa (5) the uniaxial stress component is 0.05 GPa at 4 GPa (6) during isobaric holding, the changes in the specimen pressure are negligible and the transformation proceeds under a constant driving force (7) the accuracy in the measurement of specimen resistance in 1 part in 10^3 (8) the least value of the transformed fraction that can be detected is ~0.005 (9) in the temperature experiments under pressure[11,13], the specimen temperature is maintained within ±1K.

2.6 Kinetics data

The calculation of the fraction transformed, $\zeta(t)$, as a function of time, t, is now explained using the R(p)-p data for the $\alpha \rightarrow \omega$ transformation in Ti [Fig.4(a)] and the hcp → fcc transformation in Tl [Fig.4(b)]. The Ti specimen is entirely in the α -phase prior to the transformation and in the ω–phase after the transformation is completed; R_α and R_ω denote the resistance of the Ti specimen just prior to and after the transformation. During the transformation, the specimen is an intimate random mixture of the α and ω phases; $R_m(t)$ denotes the resistance of the intermediate phase at any instant t. The fraction $\zeta(t)$ of the ω-phase as a function of time, t, is calculated from the $R_m(t)$-t data using the following equation[11] derived from the Landauer model[8]

$$\zeta(t) = \frac{\Delta r(t)}{r}\left[\frac{1+\frac{2r}{3r_\alpha}+\frac{\Delta r(t)}{3r_\alpha}}{1+\frac{\Delta r(t)}{R_\alpha}}\right] \qquad (1)$$

where $\Delta r(t) = R_m(t) - R_\alpha$ and $r = R_\omega - R_\alpha$. For the Tl specimen the suffixes α and ω are replaced respectively by hcp and fcc. The $\zeta(t)$ - t data at each desired value of p over the range 4-9 GPa for Ti, 3.3-4.6 GPa for Yb, and 3.4-4.2 GPa for Tl at 300 K are calculated from Eq(1).

The resistometric method of determining ζ has an advantage in that a small specimen (volume ~10^{-4}cm^3) is used. The volume change at the transformation is a very small fraction (a few parts in ten thousand) of the volume of the presssure transmitting medium. Therefore the specimen pressure drop as the transformation progresses is small and isobaric conditions continue to exist.

The different conductivity terms appearing in the Landauer equation are assumed to be proportional to the inverse of the respective resistances while deriving Eq(1). This amounts to neglecting the density change associated with the transformation. We have estimated[18] the error introduced in ζ by the neglect of the density change and find that the density change corrections are not more than a few percent for most of the solid-solid transformations encountered in practice.

3. RESULTS AND DISCUSSION

3.1 Magnitudes of resistance discontinuities associated with the transformation

The Ti and Yb and the Tl transformations run to completion at all pressures in the specified range. The fractional resistance increase (r/R_α) for the Ti- transformation decreases from 30% at 4 GPa to 23% at 9 GPa. This behaviour is consistent with the fact that R_ω decreases more rapidly (-0.022 GPa^{-1}) than R_α (-0.014 GPa^{-1}) with increase in pressure. Since the $\alpha \rightarrow \omega$ transformation in Ti is irreversible at 300 K, the recovered specimens after the pressure experiments were examined by X-ray diffraction. The diffractogram revealed the presence of only ω-phase. The (r/R_{fcc}) for Yb transformation increases from 86% at 3.3 GPa to 93% at 4.6 GPa. This behaviour is consistent with the

rapid increase of resistance of the fcc phase prior to the transformation with increase in pressure and also that the resistance of the bcc phase shows only a marginal decrease. The (r/R_{hcp}) values for Tl in 14 experiments over the pressure range 3.4-4.2 GPa lie between 20.5 - 23%; the average value being 21.8 ± 1%. It is seen from Fig.4(b) that the pressure dependence of the resistance of hcp and fcc phases close to the transformation are similar; the (r/R_{hcp}) values calculated from the extrapolation of AC and DE regions vary within 0.1% suggesting that (r/R_{hcp}) for Tl is independent of p.

3.2 Transformation start pressure

In continuous loading experiments (0.1 GPa min^{-1}) the onset of the Ti, Yb and Tl-transformations at 300K is observed respectively at 6,4 and 3.7 GPa. Highly reproducible values of the start pressures have been obtained by various investigators because the rates of pressurization employed do not vary widely. The present studies clearly show that these transformations can be observed over a wide range of pressures under truly isobaric conditions. The Ti, Yb and Tl-transformations have been over-driven respectively to 9, 4.6 and 4.2 GPa under a pressurization rate of 10 GPa s^{-1}. At still higher pressurization rates these transformations can be over-driven to still larger pressures provided the response times of the detection methods are commensurate with the time scale of transformation. The Bi **I** → **II** transformation (occurring at 2.55 GPa) and the fcc → bcc transformation in Yb (occurring at 4 GPa) under pressurization rates of 0.1 GPa min^{-1} have been over-driven respectively to 3 [19] and 5.5 GPa[20] by employing pressurization rates as high as[21] 10^4-10^5 GPa s^{-1}, the transformation times are respectively 8 and 25 μs. Recently, we have over-driven the Ti transformation to 13 GPa[22] where the transformation time is a few ms. These results clearly suggest that the transformation start pressure has no thermodynamic significance. The start pressure is a kinetic quantity in contrast to the equilibrium pressure which is a thermodynamic quantity. The start pressure is a function of the rate of pressurization apart from the other variables such as the specimen history, impurity levels and the nature of the high pressure environment i.e, truly hydrostatic or quasihydrostatic.

The lowest pressures at which the Ti, Yb and Tl transformations run to completion as observed in the present studies are 4, 3.3 and 3.4 GPa. While it is acceptable that a start pressure of 4 GPa for the α → ω transformation in Ti(p_o=2 GPa)[23] is greater than the thermodynamic equilibrium pressure, the start pressures of 3.3 GPa for the fcc → bcc transformation in Yb (p_o=4 GPa)[24] and 3.4 GPa for the hcp → fcc transformation in Tl (p_o=3.67 GPa)[25] are respectively lower than the accepted values of p_o. This aspect will be discussed later in this paper.

3.3 Incubation period

The Ti and the Yb transformations do not proceed as soon as the desired pressure is reached. A definite time elapses before the onset of transformation can be detected. This time is the incubation or the induction period. The feature marked by region C in Fig.3 corresponds to the incubation period. During this waiting period, t_i, the resistance of the Ti and Yb specimens remains practically constant. The pressure dependence of t_i for the Ti and Yb transformations are respectively

$$\text{Int}_i = 22.7 - 2.9\ p \qquad (2)$$

$$\text{Int}_i = 47.6 - 10.9\ p \qquad (3)$$

where t_i is in seconds and p in GPa. Typically, for Ti, t_i is 18 hours at 4 GPa and reduces to 11 seconds at 7 GPa and, for Yb, t_i is 31 hours at 3.3 GPa and reduces to 6 seconds at

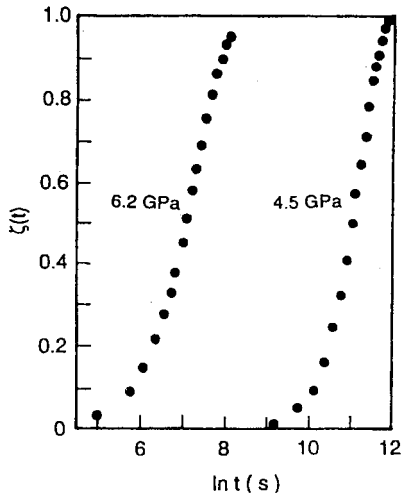

Fig. 5a.Typical kinetics data for the Ti-transformation at two different pressures.

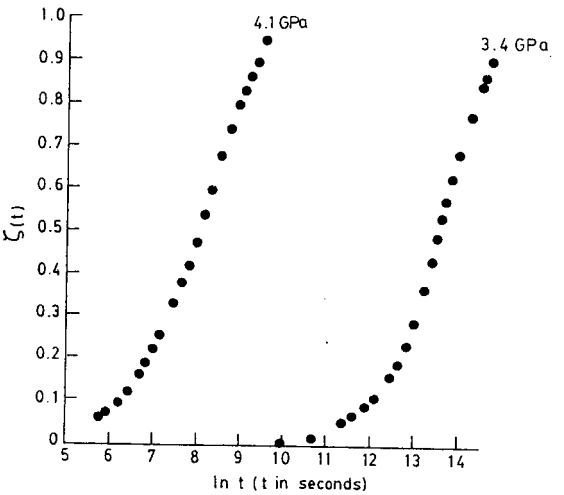

Fig. 5b. Typical kinetics data for the Yb- transformation at two different pressures.

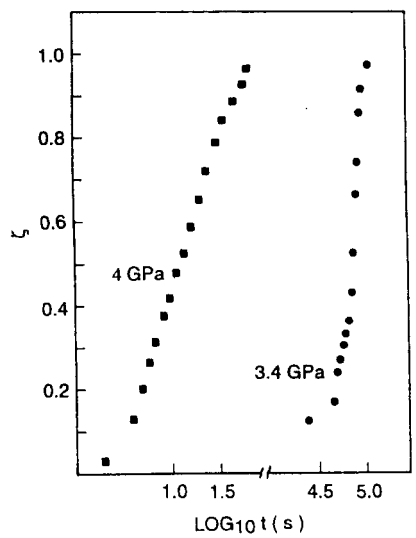

Fig. 5c. Typical kinetics data for Tl-transformation at two different pressures.

4.2 GPa. The experimentally determined t_i contains in addition to the true incubation period, the time required for a detectable fraction of the high pressure phase. In the present experiments, the smallest value of ζ is = 0.005. In contrast to the Ti and Yb transformations, the Tl transformation does not exhibit t_i i.e., the transformation begins the moment the desired pressure in the range 3.4 – 4.2 GPa is reached.

The incubation period decreasing with increasing pressure has also been observed in cadmium chalcogenides[1]. It has been suggested that the observed t_i could be an intrinsic property of the transformation or could arise as a result of time delay in pressure transmission to the specimen by a solid pressure transmitting medium. The t_i-p data [Eqs.(2) and (3)] suggest that the observed t_i in the present experiments is an inherent property of the transformation. The incubation period is a commonly observed feature of most of the isothermal phase changes. It is taken as the time required for the formation of a significant number of nuclei. The nucleation rate is believed to be transient for values of $t < t_i$ and thereafter it approaches a steady state.

3.4 ζ – t data at 300 K

The typical ζ-t data at two different pressures for the transformations under study are shown in Fig.5(a) for Ti, Fig.5(b) for Yb and Fig.5(c) for Tl. These plots are sigmoidal in nature in which ζ increases slowly at first, and then more rapidly an finally slowly again. The incubation periods are subtracted from the measured value of t for Ti and Yb transformations so that the origin of the time axis is fixed at the start of the transformation.

2.6 Kinetics data

The calculation of the fraction transformed, $\zeta(t)$, as a function of time, t, is now explained using the R(p)-p data for the $\alpha \rightarrow \omega$ transformation in Ti [Fig.4(a)] and the hcp → fcc transformation in Tl [Fig.4(b)]. The Ti specimen is entirely in the α -phase prior to the transformation and in the ω–phase after the transformation is completed; R_α and R_ω denote the resistance of the Ti specimen just prior to and after the transformation. During the transformation, the specimen is an intimate random mixture of the α and ω phases; $R_m(t)$ denotes the resistance of the intermediate phase at any instant t. The fraction $\zeta(t)$ of the ω-phase as a function of time, t, is calculated from the $R_m(t)$-t data using the following equation[11] derived from the Landauer model[8]

$$\zeta(t) = \frac{\Delta r(t)}{r}\left[\frac{1+\frac{2r}{3r_\alpha}+\frac{\Delta r(t)}{3r_\alpha}}{1+\frac{\Delta r(t)}{R_\alpha}}\right] \qquad (1)$$

where $\Delta r(t) = R_m(t) - R_\alpha$ and $r = R_\omega - R_\alpha$. For the Tl specimen the suffixes α and ω are replaced respectively by hcp and fcc. The $\zeta(t)$ - t data at each desired value of p over the range 4-9 GPa for Ti, 3.3-4.6 GPa for Yb, and 3.4-4.2 GPa for Tl at 300 K are calculated from Eq(1).

The resistometric method of determining ζ has an advantage in that a small specimen (volume ~10^{-4}cm^3) is used. The volume change at the transformation is a very small fraction (a few parts in ten thousand) of the volume of the presssure transmitting medium. Therefore the specimen pressure drop as the transformation progresses is small and isobaric conditions continue to exist.

The different conductivity terms appearing in the Landauer equation are assumed to be proportional to the inverse of the respective resistances while deriving Eq(1). This amounts to neglecting the density change associated with the transformation. We have estimated[18] the error introduced in ζ by the neglect of the density change and find that the density change corrections are not more than a few percent for most of the solid-solid transformations encountered in practice.

3. RESULTS AND DISCUSSION

3.1 Magnitudes of resistance discontinuities associated with the transformation

The Ti and Yb and the Tl transformations run to completion at all pressures in the specified range. The fractional resistance increase (r/R_α) for the Ti- transformation decreases from 30% at 4 GPa to 23% at 9 GPa. This behaviour is consistent with the fact that R_ω decreases more rapidly (-0.022 GPa^{-1}) than R_α (-0.014 GPa^{-1}) with increase in pressure. Since the $\alpha \rightarrow \omega$ transformation in Ti is irreversible at 300 K, the recovered specimens after the pressure experiments were examined by X-ray diffraction. The diffractogram revealed the presence of only ω-phase. The (r/R_{fcc}) for Yb transformation increases from 86% at 3.3 GPa to 93% at 4.6 GPa. This behaviour is consistent with the

rapid increase of resistance of the fcc phase prior to the transformation with increase in pressure and also that the resistance of the bcc phase shows only a marginal decrease. The (r/R_{hcp}) values for Tl in 14 experiments over the pressure range 3.4-4.2 GPa lie between 20.5 - 23%; the average value being 21.8 ± 1%. It is seen from Fig.4(b) that the pressure dependence of the resistance of hcp and fcc phases close to the transformation are similar; the (r/R_{hcp}) values calculated from the extrapolation of AC and DE regions vary within 0.1% suggesting that (r/R_{hcp}) for Tl is independent of p.

3.2 Transformation start pressure

In continuous loading experiments (0.1 GPa min^{-1}) the onset of the Ti, Yb and Tl-transformations at 300K is observed respectively at 6,4 and 3.7 GPa. Highly reproducible values of the start pressures have been obtained by various investigators because the rates of pressurization employed do not vary widely. The present studies clearly show that these transformations can be observed over a wide range of pressures under truly isobaric conditions. The Ti, Yb and Tl-transformations have been over-driven respectively to 9, 4.6 and 4.2 GPa under a pressurization rate of 10 GPa s^{-1}. At still higher pressurization rates these transformations can be over-driven to still larger pressures provided the response times of the detection methods are commensurate with the time scale of transformation. The Bi **I** → **II** transformation (occurring at 2.55 GPa) and the fcc → bcc transformation in Yb (occurring at 4 GPa) under pressurization rates of 0.1 GPa min^{-1} have been over-driven respectively to 3 [19] and 5.5 GPa[20] by employing pressurization rates as high as[21] 10^4-10^5 GPa s^{-1}, the transformation times are respectively 8 and 25 μs. Recently, we have over-driven the Ti transformation to 13 GPa[22] where the transformation time is a few ms. These results clearly suggest that the transformation start pressure has no thermodynamic significance. The start pressure is a kinetic quantity in contrast to the equilibrium pressure which is a thermodynamic quantity. The start pressure is a function of the rate of pressurization apart from the other variables such as the specimen history, impurity levels and the nature of the high pressure environment i.e, truly hydrostatic or quasihydrostatic.

The lowest pressures at which the Ti, Yb and Tl transformations run to completion as observed in the present studies are 4, 3.3 and 3.4 GPa. While it is acceptable that a start pressure of 4 GPa for the α → ω transformation in Ti(p_o=2 GPa)[23] is greater than the thermodynamic equilibrium pressure, the start pressures of 3.3 GPa for the fcc → bcc transformation in Yb (p_o=4 GPa)[24] and 3.4 GPa for the hcp → fcc transformation in Tl (p_o=3.67 GPa)[25] are respectively lower than the accepted values of p_o. This aspect will be discussed later in this paper.

3.3 Incubation period

The Ti and the Yb transformations do not proceed as soon as the desired pressure is reached. A definite time elapses before the onset of transformation can be detected. This time is the incubation or the induction period. The feature marked by region C in Fig.3 corresponds to the incubation period. During this waiting period, t_i, the resistance of the Ti and Yb specimens remains practically constant. The pressure dependence of t_i for the Ti and Yb transformations are respectively

$$Int_i = 22.7 - 2.9\ p \qquad (2)$$

$$Int_i = 47.6 - 10.9\ p \qquad (3)$$

where t_i is in seconds and p in GPa. Typically, for Ti, t_i is 18 hours at 4 GPa and reduces to 11 seconds at 7 GPa and, for Yb, t_i is 31 hours at 3.3 GPa and reduces to 6 seconds at

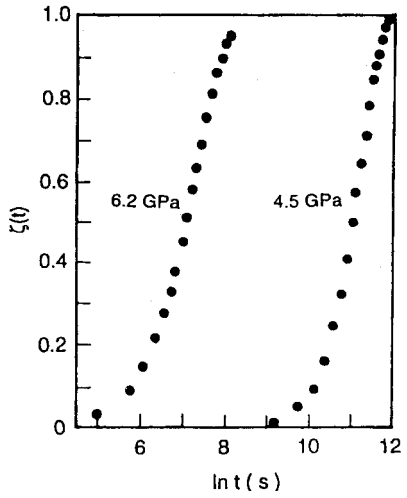

Fig. 5a.Typical kinetics data for the Ti-transformation at two different pressures.

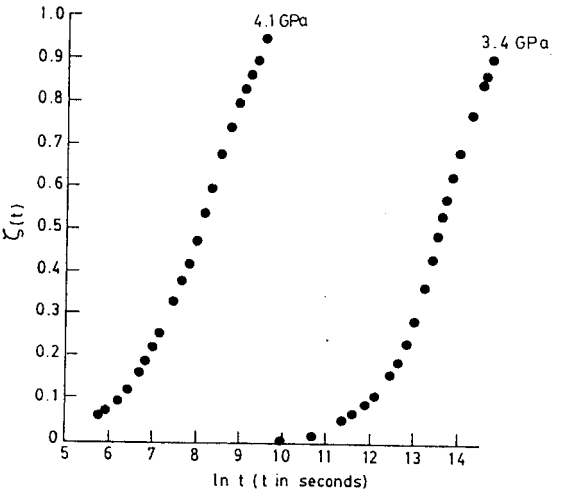

Fig. 5b. Typical kinetics data for the Yb- transformation at two different pressures.

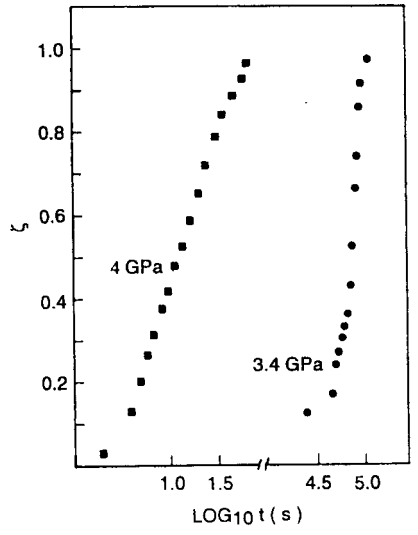

Fig. 5c. Typical kinetics data for Tl-transformation at two different pressures.

4.2 GPa. The experimentally determined t_i contains in addition to the true incubation period, the time required for a detectable fraction of the high pressure phase. In the present experiments, the smallest value of ζ is = 0.005. In contrast to the Ti and Yb transformations, the Tl transformation does not exhibit t_i i.e., the transformation begins the moment the desired pressure in the range 3.4 – 4.2 GPa is reached.

The incubation period decreasing with increasing pressure has also been observed in cadmium chalcogenides[1]. It has been suggested that the observed t_i could be an intrinsic property of the transformation or could arise as a result of time delay in pressure transmission to the specimen by a solid pressure transmitting medium. The t_i-p data [Eqs.(2) and (3)] suggest that the observed t_i in the present experiments is an inherent property of the transformation. The incubation period is a commonly observed feature of most of the isothermal phase changes. It is taken as the time required for the formation of a significant number of nuclei. The nucleation rate is believed to be transient for values of $t < t_i$ and thereafter it approaches a steady state.

3.4 ζ – t data at 300 K

The typical ζ-t data at two different pressures for the transformations under study are shown in Fig.5(a) for Ti, Fig.5(b) for Yb and Fig.5(c) for Tl. These plots are sigmoidal in nature in which ζ increases slowly at first, and then more rapidly an finally slowly again. The incubation periods are subtracted from the measured value of t for Ti and Yb transformations so that the origin of the time axis is fixed at the start of the transformation.

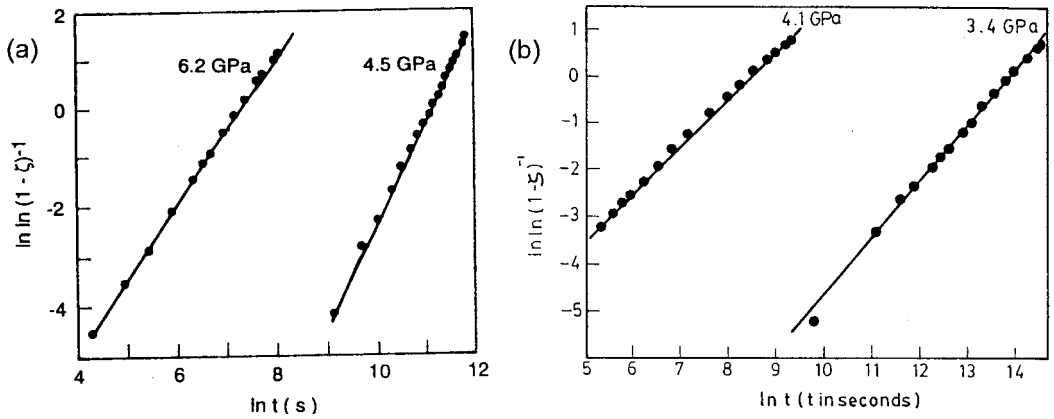

Fig. 6. Linear lnln (1– ζ)$^{-1}$ versus lnt plots typical of (a) Ti- and (b) Yb-transformations.

The ζ-t plots shift to lower time scales along the logarithmic time axis with increasing pressure indicating that the kinetics of the transformation becomes faster as the pressure increases. The time dependent nature of the transformation under a constant driving force suggests a thermally activated nucleation and growth as the operative mechanism.

The ln ln(1-ζ)$^{-1}$ versus lnt plots corresponding to the ζ-t data shown in Figs. 5(a) and 5(b) are shown in Figs. 6(a) and 6(b) and are linear; the co-efficient of determination is 0.999. Such linear plots are obtained for all the ζ-t data at different pressures for both Ti and Yb. This suggests that the ζ-t data satisfy the standard form of Johnson-Mehl Avrami equation:

$$\zeta(t) = 1 - \exp\left(\frac{t}{\tau}\right)^n \tag{4}$$

where the characteristic time τ and the JMA exponent n are constants at a given p. The slope of the ln ln(1-ζ)$^{-1}$ versus lnt line gives the value of n and from the intercept, lnτ can be determined. However, the ln ln(1-ζ)$^{-1}$ verus lnt data for the Tl-transformation do not fall on a single straight line.The pressure dependence of n for the Ti-transformation over the range 4-9 GPa is of the form

$$n = 1.52 + 0.26\,p - 0.035\,p^2 \tag{5}$$

and for the Yb-transformation over the pressure range 3.3-4.6 GPa it is of the form

$$n = 1.36 + 0.55\,p - 0.17\,p^2 \tag{6}$$

where p is in GPa. Typically, for Ti, n = 2 ± 0.1 at 5 GPa and decreases to 1 ± 0.1 at 9 GPa. Similar values for Yb are n = 1.5 ± 0.2 at 3.3 GPa and decreases to 0.4 ± 0.1 at 4.5 GPa.The kinetics of transformations occurring at a constant driving force (isothermal, isobaric or isothermal-isobaric conditions) involving nucleation and growth processes are often described using the JMA equation[26]. The values of n that are obtained under different conditions of nucleation and growth have been described earlier[4]. For a constant nucleation rate, the values of n obtained are 4,3 and 2 corresponding to 3-,2- and 1-dimensional growth. In case of the growth of pre-existing nuclei, n = 3, 2 and 1 respectively for 3-,2- and 1-dimensional growth. It is important to note that in the frame

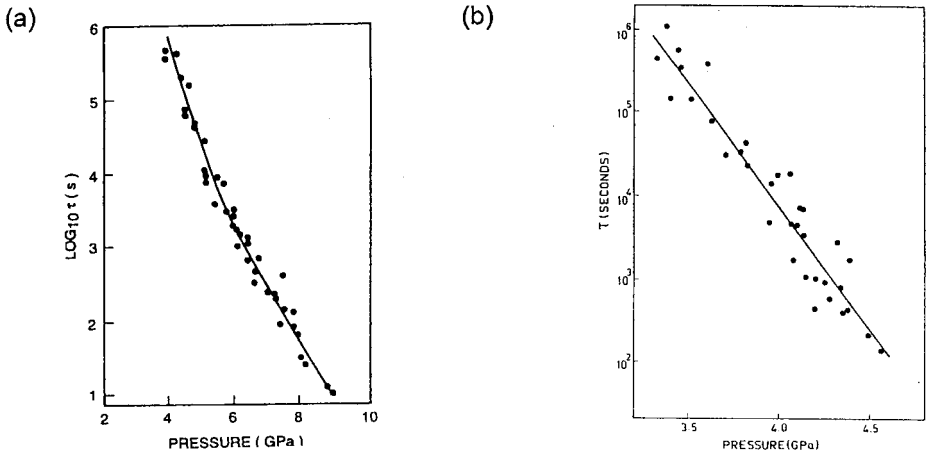

Fig. 7. Pressure dependence of τ at 300 K for (a) Ti- and (b) Yb transformations.

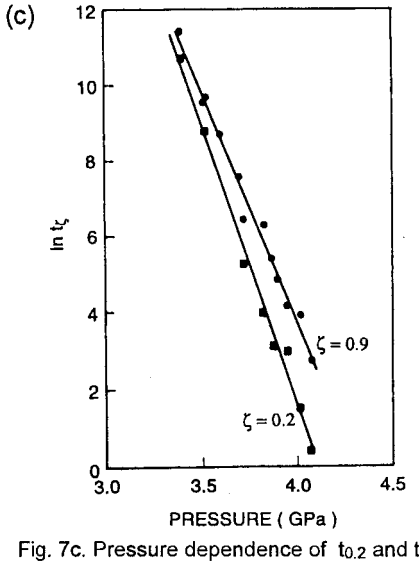

Fig. 7c. Pressure dependence of $t_{0.2}$ and $t_{0.9}$ for Tl-transformations.

work of JMA theory, the lowest value is of n = 1. The factors leading to the occurrence of n < 1 have been examined[4] and it has been suggested that either some of the assumptions underlying the JMA theory are not valid, or a new situation with regard to impingement of growing regions develops which is not envisaged in the JMA theory. Further, it has also been shown[4] that Eq.(4) is valid only if the nucleation rate I(t) which appears in the general form of the Avrami equation

$$-\ln(1-\zeta) = sg^k \int_0^t I(t)(t-t')^k dt' \qquad (7)$$

is of the form ct^{m-1} where m > 0. In Eq(7), s and k denote respectively the shape factor and the dimensionality of the growth process and $sg^k(t-t')^k$ represents the volume at time t of a given nucleus which originated at t and g is the isotropic growth rate. The fact that ln $\ln(1-\zeta)^{-1}$ versus lnt data for Tl does not satisfy the standard form of JMA equation should not be taken to indicate that the hcp → fcc transformation does not proceed via nucleation and growth processes. In fact, the time dependence of the transformation under isobaric conditions [Fig.5(c)] points to a thermally activated nucleation and growth mechanism.

3.5 Analysis of lnτ– p data

It is seen from Eq.(4) that when t = τ, $\zeta = 1-e^{-1} = 0.63$ and τ is the time required for 63% transformation. The values of τ at different pressures in the range 4-9 GPa for Ti and 3.3-4.6 GPa for Yb are calculated from the ζ-t data. The lnτ - p data for the Ti- and Yb-transformations at 300K are shown in Figs.7(a) and 7(b) respectively. Since the analysis of the lnτ - p data does not depend upon whether the kinetics of the transformation is governed by Eq.(4), similar data for the Tl-transformation i.e. $\ln t_\zeta$-p data at ζ=0.2

mation is governed by Eq.(4), similar data for the Tl-transformation i.e. $\ln t_\zeta$-p data at ζ=0.2 and 0.9 are shown in Fig.7(c). With increasing pressure, τ or in general t_ζ decreases exponentially indicating that the kinetics of the transformations becomes faster. A detailed analysis of these data has been described in earlier publications[11,13,16].

The ln τ-p data for Ti in the pressure range 6-9 GPa can be approximated to be linear, whereas the data for Yb and Tl are linear over the entire range of pressures. A linear regression analysis of the data gives the following equations respectively for Ti, Yb and Tl:

$$\ln \tau = 17.56 - 1.674\, p \quad (8)$$

$$\ln \tau = 36.2 - 6.8\, p \quad (9)$$

$$\ln t_{0.9} = 52.7 - 12.2\, p \quad (10)$$

where τ ($t_{0.9}$) are in seconds and p in GPa.

For a transformation involving a thermally activated nucleation and growth mechanism, the time t_ζ, required for a fraction ζ is given by[4,11,13,16]

$$\ln t_\zeta = b(\zeta) + (\Delta G^*(p)/RT) \quad (11)$$

where $b(\zeta)$ is a term depending only on ζ and $\Delta G^*(p)$ is a pressure dependent activation energy barrier for the transformation. The activation volume ΔV^* is given by

$$\Delta V^* = \left[\frac{\partial(\Delta G^*)}{\partial P}\right]_T \quad (12)$$

Combining Eqs.(11) and (12), ΔV^* is expressed as

$$\Delta V^* = RT\left(\frac{\partial(\ln t_\zeta)}{\partial P}\right) \quad (13)$$

Using Eq(13), ΔV^* calculated from the slope of the lnτ-p line is -4.2, -17, -30.5 cm^3/mol at 300K respectively for Ti-, Yb- and Tl-transformations.

It is clear from the present data, that the extent of over-driving the transformation on the pressure scale decreases in the following order: 9 GPa for Ti, 4.6 GPa for Yb and 4.2 GPa for Tl. Considering that ΔV^* for Tl is the largest as compared to those of Ti and Yb, it appears that transformations with a large, ΔV^* cannot be over-driven to large extents. Similar arguments apply to the Bi **I** $\rightarrow$ **II** transformation, whose p_o = 2.55 GPa, which has been over-driven only upto 3 GPa[19] where the transformation times are already as small as 8 μs[19] suggesting that the Bi **I** $\rightarrow$ **II** transformation is expected to have a large ΔV^*. It is well known that Bi **I** $\rightarrow$ **II** and Tl hcp $\rightarrow$ fcc transformations are used as fixed points for the measurement of pressure up to 4 GPa. It appears, that, for a choice of a solid-solid phase transformation as a fixed point in the measurement of pressure, apart from other requirements[27], the transformation possesses a large ΔV^* so that it cannot be over-driven to large extents even under high pressurization rates.

The ΔV^* is found to depend on the choice of t_ζ . For the Ti-transformation, ΔV^* is -4.8, -4.2 and -4.1 cm^3mol^{-1} respectively for ζ = 0.3, 0.63 and 0.8. For the Yb transformation,

ΔV^* is -22, -17 and -15 $cm^3\ mol^{-1}$ respectively for ζ = 0.1, 0.63 and 0.9. For the Tl-transformation, ΔV^* is -37 and -30.5 $cm^3\ mol^{-1}$ respectively for ζ = 0.2 and 0.9. Interestingly, for the transformations under study, the magnitude of ΔV^* decreases with increase in ζ.

The $\ln\tau$ - p data for Ti exhibit a curvature at 6 GPa. On fitting through the $\ln\tau$ - p data on equation of the form (whose basis has been discussed in a later section)

$$\ln \tau = a_1 + a_2(p - p_o) + a_3(p - p_o)^{-q} \tag{14}$$

the following values are obtained: a_1 = 13.36, a_2 = -1.51 GPa^{-1}, a_3 = 23.7 $(GPa)^2$, p_o = 1.47 GPa and q=2. The continuous curve shown in Fig.7(a) is drawn using Eq.(14). The Yb and Tl data do not exhibit this curvature even at pressures as low as 3.3 and 3.4 GPa. It may be noted that τ = 263 hours at 3.3 GPa for Yb and $t_{0.9}$ = 21 hours at 3.4 GPa for Tl. At p = 3.2 GPa, Tl-transformation did not start even after a waiting period of 240 hours. Isobaric holding at pressures lower than these values are impractical and hence were not attempted.

3.6 Energetics of the transformations

The activation energy barrier $\Delta G^*(p)$ appearing in Eq.(11) is a weighted average of the activation free energies of the nucleation and growth processes. The weightage in general, depends on the exact laws controlling the nucleation and growth processes. Eq.(11) is re-written as

$$\ln t_\zeta = b - \frac{\Delta S^*}{R} + \frac{\Delta H^*}{RT} = b_0 + \frac{\Delta H^*}{RT} \tag{15}$$

Where b_o = b- ($\Delta s^*/R$), and Δs^* and ΔH^* are respectively the activation entropy and enthalpy. Eq.(15) suggests that ΔH^* can be experimentally determined if t_ζ is measured as a function of T. Such measurements, under isobaric-isothermal conditions, are made for Ti at 5,7, and 8 GPa, for Yb at 3.3, 3.6 and 3.8 GPa and for Tl at 3.5 GPa and at each pressure, the temperature dependence of $\tau(t_{0.9})$ is obtained over a range 300-365 K. The details of the heating arrangement, sequence of steps followed in reaching a desired value of p and T have been described elsewhere[11,13,17].

The high temperature ζ - t data exhibit features similar to those observed at room temperature. For instance, the transformations in Ti and Yb are preceded by t_i and the ζ-t data satisfy JMA equation. However, for Tl, no t_i is observed and ζ-t data do not satisfy JMA equation. The $\ln\tau$ versus (1/T) plots at different pressures are shown in Fig.8(a) for Ti and 8(b) for Yb. It is seen from these data, that, at a given p, τ decreases with increase in T indicating that the kinetics of the transformations are enhanced at higher T. This clearly establishes that the transformations are thermally activated. The activation enthalpies, ΔH^*, obtained from the slopes of these lines are shown in Figs.9(a) for Ti and 9(b) for Yb. The ΔH^* values lie in the range 10-15 kcal/mole for the Ti-transformation and 15-20 kcal/mole for the Yb-transformation. A similar analysis of the temperature dependence of $t_{0.9}$ for the Tl-transformation at 3.5 GPa indicates that the kinetics of the hcp → fcc transformation is enhanced at higher temperatures confirming a thermally activated nucleation and growth as the operating mechanism. A linear fit to the $t_{0.9}$ versus 1/T data gives ΔH^* = 22.6 kcal/mol at 3.5 GPa.

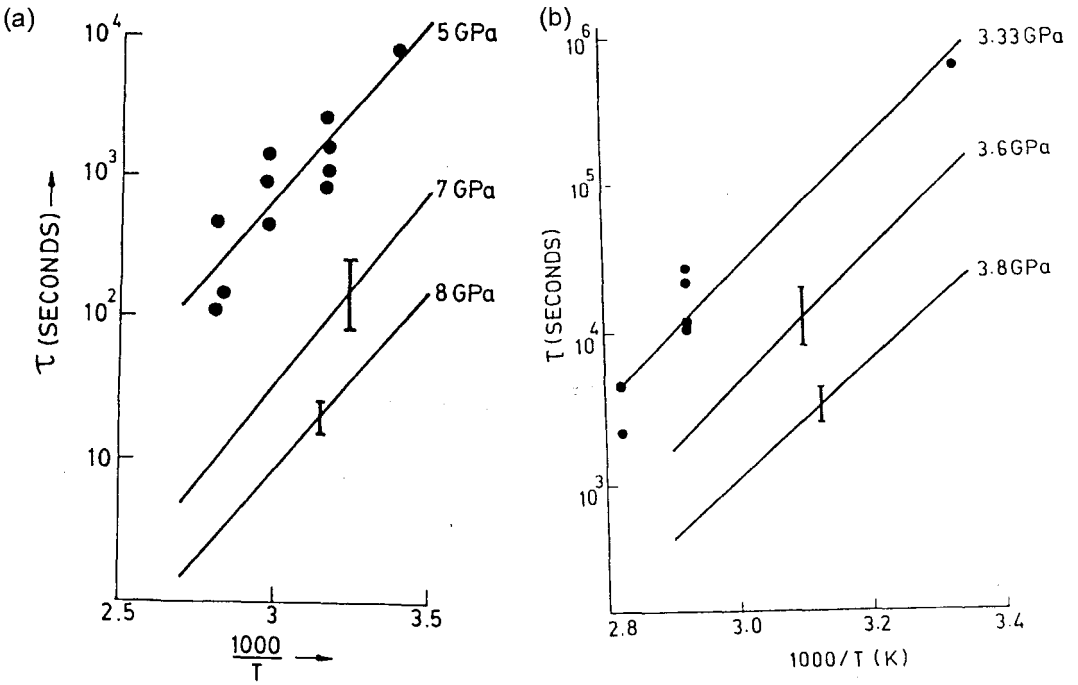

Fig. 8. Temperature dependence of τ for (a) Ti- and (b) Yb-transformations at different pressures.

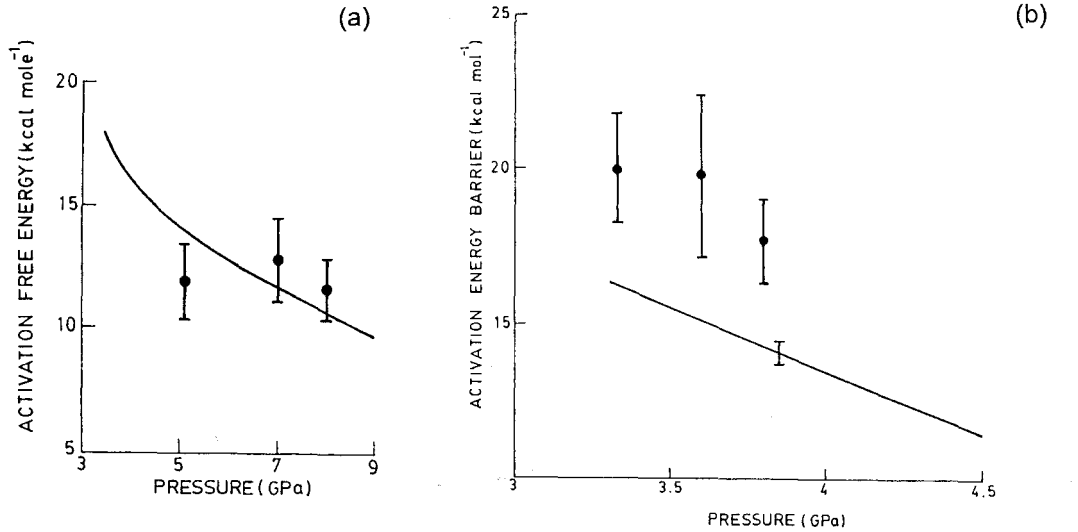

Fig. 9. Pressure dependence of the activation energy barrier obtained using b= -13.8 in (a) Eq.19 for Ti- and (b) Eq.20 for Yb-transformations. The activation enthalpies obtained from the slopes of ln τ versus 1000/T lines [Fig.8(a),(b)] are shown by dots.

The values of b_0 determined from the intercepts of the lnτ ($t_{0.9}$) versus 1/T line are on an average -14.2 for Ti(5-8 GPa), -20.5 for Yb (3.3-3.8 GPa) and -28 for TI(3.5 GPa). With these values of b_o, and combining Eq.(15) with Eqs.(14), (9) and (10) the following equations are obtained respectively for Ti, Yb and TI:

$$\Delta H^* = RT\,[29.8 - 1.51p + 23.7\,(p - 1.47)^{-2}] \quad (16)$$

$$\Delta H^* = RT\,[56.7 - 6.8p] \quad (17)$$

$$\Delta H^* = RT\,[80.7 - 12.2p] \qquad (18)$$

Eqs.(16-18) are obtained by using the pressure dependence of the kinetics of the transformations at 300K and b_o obtained from the independent measurements of the temperature dependence of the kinetics. It is to be noted that ΔH^* values obtained from the slopes of $\ln\tau(t_{0.9})$ versus 1/T lines are not used. These equations give ΔH^*=10.9 – 14.3 kcal mol^{-1} for Ti in the pressure range 5 - 8 GPa, 18.3 - 20.4 kcal mol^{-1} for Yb in the pressure range 3.3 - 3.8 GPa, and 22.6 kcal mol^{-1} for Tl at 3.5 GPa in excellent agreement with the values obtained from independent measurements of the temperature dependence of $\tau(t_\zeta)$. This amply justifies the use of Eq.(15) in the analysis of the present kinetics data.

Alternatively, combining Eq.(11) with Eqs.(14), (9) and (10) leads to:

$$\Delta G^* = RT\,[-b + 15.58 - 1.51\,p + 23.7(p\text{-}1.47)^{-2}] \qquad (19)$$

$$\Delta G^* = RT\,[-b + 36.2 - 6.8\,p] \qquad (20)$$

$$\Delta G^* = RT\,[-b + 52.7 - 12.2\,p] \qquad (21)$$

respectively for Ti, Yb and Tl transformations. Eqs.(19)-(21) differ from Eqs.(16-(18) in that ΔG^* replaces ΔH^* and the parameter b is not experimentally obtained. The pressure dependence of ΔG^* can be estimated using Eqs. (19)-(21) provided the value of b is known. It is seen from Eq.(11) that the minimum value of $\ln t_\zeta$ = b i.e. $\Delta G^*(p) = 0$. In the absence of any activation energy barrier, it is reasonable to expect that the transformation will propagate with the velocity of sound in a solid, which is typically a few kms^{-1}. Under these conditions, τ is the order of a microsecond and b= $\ln(10^{-6})$ = -13.8. The values of ΔG^* calculated from Eqs.(19) and (20) are shown by solid lines in Figs.9(a) and 9(b) respectively. For Tl, ΔG^*=14.1 kcal mol^{-1} at 3.5 GPa as compared to ΔH^* = 22.6 kcal mol^{-1}. The differences between ΔG^* and ΔH^* arise because of the $T\Delta s^*$ term. This analysis shows that the activation energy barrier, ΔG^*, for the transformations under study decrease with increase in pressure. Consequently, the kinetics of the transformation is enhanced at higher pressures.

Using b_o = b - (Δs^*/R) with b_o = -14.2, -20.5 and -28 (determined experimentally) respectively for Ti, Yb and Tl transformations, and b = -13.8, the values of Δs^* respectively are 0.8, 13.3 and 27.3 cals $mol^{-1}k^{-1}$.

3.6 Thermodynamic equilibrium pressure (p_0)

The thermodynamic equilibrium pressure of a pressure induced transformation is often determined by assuming that it is located at the midpoint of a hysteresis loop, or equivalently by assuming that it is the average of the start pressures of the forward (p_f) and reverse (p_r) transformations. On the basis of many experimental studies [27], it has been pointed out that this assumption is not correct, and in fact p_0 is often higher than the value obtained by this assumption. In this section, we briefly discuss the estimates of p_0 for the Ti, Yb and Tl-transformations on the basis of the considerations of the kinetics of these transformations.

3.6.1 $\alpha \leftrightarrow \omega$ transformation in Ti

In the case of Ti, ω-phase is retained metastably even after the pressure is released to one atmosphere at 300K and therefore it is not possible experimentally to determine p_0 as the average of p_f and p_r. The methods of determining p_0 for the Ti-transformation have been discussed earlier[4] and the value of p_0 obtained by these methods [28] is 2 GPa at

300K. The In τ -p data at 300K for Ti[Fig.7(a)] exhibit a curvature at 6 GPa. It is reasonable to assume that $t \rightarrow \infty$ as $p \rightarrow p_0$. Thus, a single curve passing through the data points in the entire range of pressures 4-9 GPa has as asymptotes the lines $p=p_0$ and a line nearly parallel to the line given by Eq.(8). A general equation (Eq.14) satisfies these conditions. The iterative method used to fit Eq.(14) to the ln-p data for different integral values of q has been discussed earlier[11]. This analysis gives p_0 = 1.5 GPa for q=2 in excellent agreement with the values of p_0 obtained experimentally.

3.6.2 fcc $\leftrightarrow$ bcc transformation in Yb

In continuous loading experiments (0.1 GPa min^{-1}) at 300K it has been observed[29] that on compression, the fcc $\rightarrow$ bcc transformation occurs at p_f = 3.95 GPa, and on de-compression, the bcc $\rightarrow$ fcc transformation occurs at p_r=1 GPa. However, p_0 for this transformation has been believed to be close to 4 GPa ie., to p_f. The Inτ-p data [Fig.7(b)] clearly show that the fcc $\rightarrow$ bcc transformation occurs at pressures as low as 3.3 GPa. Since a pressure induced transformation can occur only at a $p_f > p_0$, p_0 for Yb has to be less than 3.3 GPa.

We have suggested a method[15] to determine p_0 by measuring the pressure and temperature dependence of the kinetics ($Int_{0.9}$ versus p data) of both the forward (fcc $\rightarrow$ bcc) and the reverse (bcc $\rightarrow$ fcc) transformations under isobaric-isothermal conditions. From the kinetics data at 300K, we obtain the activation volumes of both the forward (ΔV^*_f) and the reverse (ΔV^*_r) transformations. From the kinetics data at high temperatures, the activation enthalpies of the forward (ΔH_f^* at a known p_f) and the reverse (H_r^* at a known p_r) transformations are obtained. Using these results, the pressure dependence of the activation energy barrier for the forward (ΔG_f^*) and reverse (ΔG_r^*) transformations are obtained. p_0 is taken as that pressure at which $\Delta G_f^* = \Delta G_r^*$ and thereby we obtain p_0 = 2.9 GPa for the Yb transformation at 300K.

3.6.3 hcp $\leftrightarrow$ fcc transformtion in Tl

The average of the reported values[30-33] of p_0 for the Tl-transformation at 300K is 3.68±0.03 GPa. Typically, Kennedy and La Mori[32] obtain a start pressure of the forward transformation as 3.682 GPa and that of the reverse transformation as 3.656 GPa, and p_0 = 3.669 GPa. We have measured the kinetics of the forward transformation (hcp $\rightarrow$ fcc) down to 3.4 GPa, and therefore we expect p_0 to be less than 3.4 GPa. If $p_0 < 3.4$ GPa, then the occurrence of the reverse transformation (fcc $\rightarrow$ hcp) at 3.656 GPa[32] is puzzling. This will mean that on decompression from a region where the fcc phase is stable, the hcp phase appears above p_0 i.e, in the pressure region where the fcc phase is stable. The bcc $\leftrightarrow$ hcp transformation in Fe[34] also exhibits a similar behaviour[16]. Bridgman[35] observed the hcp $\rightarrow$ fcc transformation in Tl at 2.5 GPa in shearing experiments. While shear stresses affect both p_f and p_r (ΔG^* reduces in the presence of shear stresses) it is not clear whether p_0 is also affected. The earlier work on $\alpha \rightarrow \omega$ transformation in Ti[28] and on some re-constructive transformations[36] suggest that p_0 is not altered by the shear stresses. What is altered is the hysteresis-width of the transformation. Following this view, p_0 for the Tl-transformation is ~2.5 GPa. In such a case, the occurrence of the transformation at 3.4 GPa in our studies stands explained. Alternatively, it is to be noted that the Tl-specimen in the present experiments is embedded in talc, and therefore the shear stresses are limited by the shear strength of talc. An estimate of the shear strength of talc from radial pressure gradients and the thickness of the talc gives a value of 0.025 GPa at 4 GPa and a uniaxial stress component of 0.05 GPa. If the difference between the present value (3.4 GPa) and the accepted value of p_0(3.68 GPa) is attributed to the

presence of a uniaxial stress component, then a shift is ~ 0.3 GPa in p_0 must arise from a uniaxial stress component of ~ 0.05 GPa.

4. CONCLUSIONS

(a) A high pressure resistivity cell useful up to 10 GPa and 300-370K, and a rapid pressurization facility ($10GPas^{-1}$) suitable for obtaining the kinetics data, under isobaric-isothermal conditions, of pressure-induced displacive type phase transformations in metallic materials have been developed.

(b) The Ti and the Yb-transformations are preceded by an incubation period which decreases exponentially with increase in pressure, and the kinetics data satisfy the standard form of JMA equation. However, the Tl-transformation does not exhibit these features.

(c) The kinetics of these transformations exhibit features characteristics of a transformation involving thermally activated nucleation and growth.

(d) The enhancement of the kinetics of these transformations at higher pressures is due to the decrease in activation energy barrier for the transformation with increase in over-pressure.

(e) The thermodynamic equilibrium pressure for the Ti-, Yb-, and Tl- transformations obtained from the analysis of the kinetics data are respectively 2, 2.9 and < 3.4 GPa at 300 K.

ACKNOWLEDGEMENTS

I thank Dr. A. K. Singh for introducing me to the various aspects of the kinetics of pressure induced solid-solid phase transformations. The work on Ti and Yb transformations forms a part of my Ph.D work which was carried out under his supervision.

REFERENCES

1. Onodera, A., Rev. Phys. Chem. Japan, 1971,**41**, 1.
2. Osugi, J., Hara, K. and Katayama, M, Bull, Inst. Chem. Res. (Kyoto University), 1975, **53**, 269.
3. Singh, A. K., Bull. Mat .Sci., 1983, **5**, 219.
4. Singh, A.K., Mater.Sci.Forum, (Trans Tech-Switzerland), 1985, **3**, 291.
5. Murali Mohan, Kinetics of pressure induced phase transformations in solids, Ph.D Thesis, Bangalore University, 1992.
6. Singh, A.K, Divakar, C. and Murali Mohan, Rev. Sci. Instrum., 1983, **54**, 1407.
7. Murali Mohan and Singh, A.K., PD-MT-8911, (Internal Report-NAL),1989.
8. Landauer, R., J. Appl. Phys., 1952, **23**, 779.
9. Murali Mohan, Divakar, C. and Singh, A.K., Trans. Ind. Inst.Met., (Special Issue), 1982, **35**, 1.
10. Singh, A. K., Murali Mohan, and Divakar, C., J. Appl. Phys., 1982, **53**, 1221.
11. Singh, A. K., Murali Mohan, and Divakar, C., J. Appl. Phys., 1983, **54**, 5721.
12. Singh, A. K., Mohan, M. and Divakar, C., Mater. Res. Soc. Symp. Proc. 1984, **22**, 77.
13. Divakar, C., Murali Mohan, and Singh, A.K., J. Appl. Phys., 1984, **56**, 2327.

14. Divakar, C., Murali Mohan, and Singh, A.K., J. Instrum. Soc. India, 1985, **15**, 1.
15. Mohan, M., Divakar, C., and Singh, A.K., Physica, 1980, **139**, and **140B**, 253.
16. Murali Mohan and Singh, A.K., in: Advances in High Pressure Science and Technology, Ed., Anil K.Singh, (Tata McGraw-Hill), 1995, 121.
17. Murali Mohan and Anil K.Singh, in: High Pressure Science and Technology, Ed., W. A. Trzeciakowski, Proc.of the Joint XV AIRAPT and XXXIII EPRG Int. Conf. 1996, 390.
18. Murali Mohan and Anil K.Singh, in: Recent Trends in High Pressure Research, Proceedings of the XIII AIRAPT International Conference on High Pressure Science and Technology, Ed., Anil K.Singh, 1992, 913.
19. Singh, A. K., High Press. Res., 1990, **4**, 336.
20. Singh, A. K., in: Recent Trends in High Pressure Research, Ed., A. K. Singh, 1992, 313.
21. Singh, A. K., Rev. Sci. Instrum. 1989, **60**, 253.
22. Murali Mohan and Singh, A. K., (unpublished)
23. ZilBershteyn, V.A, Nosova, G.I, and Estrin, E.I., Phys .Met .Metallogr. (USSR), 1974, **35**, 128.
24. Souers, P. , and Jura, G., Science, 1963, **140**, 481.
25. Boyd, F. R., and England, J. L., J. Geophys. Res., 1960, **65**, 741.
26. Christian, J. W., The Theory of Transformations in: Metals and Alloys, Part I, Equilibrium and General Kinetics Theory, (Pergamon-Oxford), 1975, Chapter 1.
27. Decker, D. L., Bassett, W. A., Merrill, L., Hall, H. T., and Barnett, J. D., J. Phys. Chem. Ref. Data. 1972, **1**, 773.
28. Zil'Bershteyn, V. A., Chistotina, N. P., Zharov, A. A., Grishina, N. S., and Estrin, E. I., Phys. Met. Metallogr. (USSR), 1976, **39**, 208.
29. Hall, H. T., and Merrill, L., Inorg. Chem., 1963, **2**, 618.
30. Adler, P. N., and Margolin, H., Trans. Metall. Soc. AIME, 1964, **230**, 1048.
31. Kennedy, G. C., and LaMori, P. N., in: Progress in very high pressure research, Eds., F. P. Bundy, W. R. Hibbard and H. M. Strong, (John Wiley-New York), 1961, 304.
32. Kennedy, G. C., and LaMori, P. N., J. Geophy. Res., 1962, **67**, 851.
33. Zeto, R. J. and Vanfleet, H. B., J. Appl. Phys., 1969, **40**, 2227.
34. Huang, E., Bassett, W.A., and Tao, P., in: High Press. Res. in Min. Phy., Eds., M .H Manghnani and Syono, Y, (Terra Scientific American Geophysical Union), 1987, 165.
35. Bridgman, P.W., Phys.Rev. 1935, **48**, 893.
36. Dachille, F. and Roy, R., in: Reactivity of Solids, Ed., J. de Boer, (Elsevier-Amsterdam), 1961, 502.